First Demonstration of Selective Triplet Quenching in the Radical−Triplet Pair Mechanism (RTPM) of Chemically Induced Dynamic Electron Polarization (CIDEP)

Guanglong He,[†] Ciping Chen,[‡] Junlin Yang,[†] and Guangzhi Xu*[,†]

State Key Laboratory for Structural Chemistry of Stable and Unstable Species, Institute of Chemistry, Academia Sinica, Beijing 100080, People's Republic of China, and Institute of Photographic Chemistry, Academia Sinica, Beijing 100101, People's Republic of China

Received: December 10, 1997

Emissive chemically induced dynamic electron polarization (CIDEP) signals produced through the interaction between the lowest excited triplet phenothiazine (^{3}PTH) and 2,2,6,6-tetramethylpiperidinyloxyl (TEMPO) radical were detected by the time-resolved electron spin resonance (TRESR) method. The emissive spin polarization can be explained by the radical−triplet pair mechanism (RTPM). The fluorescence quenching and photoacoustic calorimetric experiments demonstrate directly that the emissive CIDEP signal is generated by the quartet spin states of the radical−triplet pair surviving through spin selective triplet quenching in the doublet spin states of the radical−triplet pair.

1. Introduction

Since the discovery of chemically induced dynamic electron spin polarization (CIDEP) by Fessenden and Schuler,[1] CIDEP has been widely used to study photochemical and photophysical processes, and much information such as determination of reaction mechanisms, identification of transient radical intermediates that are undetectable using other methods, and measurement of radical spin−lattice relaxation times, precursor triplet dynamic properties, radical ion-pair interaction, and relative reaction rates[2,3] may be obtained.

There are three main mechanisms to generate CIDEP on radicals. First is the triplet mechanism (TM), in which the electron spin polarization of a reaction precursor triplet state is preserved in produced radicals.[2−4] Second is the radical pair mechanism (RPM), which is caused by the mixing of singlet (S) and triplet (T) spin states of a radical pair.[2,3,5−7] Third is the radical triplet pair mechanism (RTPM), in which a quartet or a doublet pair spin state from the encounter of a triplet molecule and a radical may be formed. The doublet encounters can undergo triplet quenching, and the radicals will leave those encounters unpolarized. The remaining quartet pair states experience radical−triplet interactions, altering the spin populations with time. If quartet−doublet mixing by zero-field splitting (zfs) and quartet−doublet splitting by the exchange interaction are considered, the resulting radical will give total emissive or absorptive CIDEP signals according to $J > 0$ or $J < 0$.[8] Furthermore, if quartet−doublet mixing by hyperfine (hf) interaction in addition to zero-field splitting (zfs) is taken into account, the resulting radical will give E+E/A type CIDEP on radicals. This is the so-called quartet precursor RTPM.[9−11] On the other hand, the random encounter of the lowest excited singlet molecule and radical yields the doublet spin states of the pair. In this pair enhanced ISC caused by the radical occurs and doublet spin states of pairs between radicals and triplet molecules are formed. Hence the doublet spin states of the pairs are initially populated much more than quartet spin states, which is opposite of the quartet precursor RTPM, and CIDEP generated in radicals is A+AtE type. This is the so-called doublet precursor RTPM.[9−11]

The interaction between excited molecules and radicals is often observed as EISC (enhanced intersystem crossing) or triplet quenching with radicals by means of fluorescence and phosphorescence spectroscopy.[12−16] However, no work has been reported on the triplet quenching utilizing the pulse laser photoacoustic calorimetric technique as far as we know. To obtain a deeper understanding of RTPM, in this paper TRESRS, fluorescence spectroscopy, and pulse laser photoacoustic calorimetry have been used to investigate the photoinduced spin polarization transfer process in the phenothiazine (PTH)−2,2,6,6-tetramethylpiperidinyloxyl (TEMPO) system. The results obtained provide the first direct demonstration of the selective triplet quenching in RTPM proposed by Blätter et al.[8]

2. Experimental Section

Acridine and phenothiazine (PTH) were recrystallized from ethanol several times respectively. Ethylene glycol (RH) was distilled two times. Anthracene (AN) was sublimated several times. 2,2,6,6-Tetramethylpiperidinyloxyl (TEMPO) (Aldrich) was used as received.

The X-band TRESR spectrometer with a time resolution of 200 ns was described elsewhere.[17] The experimental arrangement comprised a Nd:YAG laser (355 nm, 20 ns pulse width, 10 mJ/pulse energy, 20 Hz repetition frequency), a boxcar integrator (EG&G4400-1), and a digital oscilloscope (HP5460). The transient ESR signals obtained without magnetic field modulation were transferred to the boxcar integrator for spectrum measurements and to the digital oscil-

* Corresponding author.
[†] Institute of Chemistry.
[‡] Institute of Photographic Chemistry.

S1089-5639(98)00490-3 CCC: $15.00
Published on Web 04/04/1998

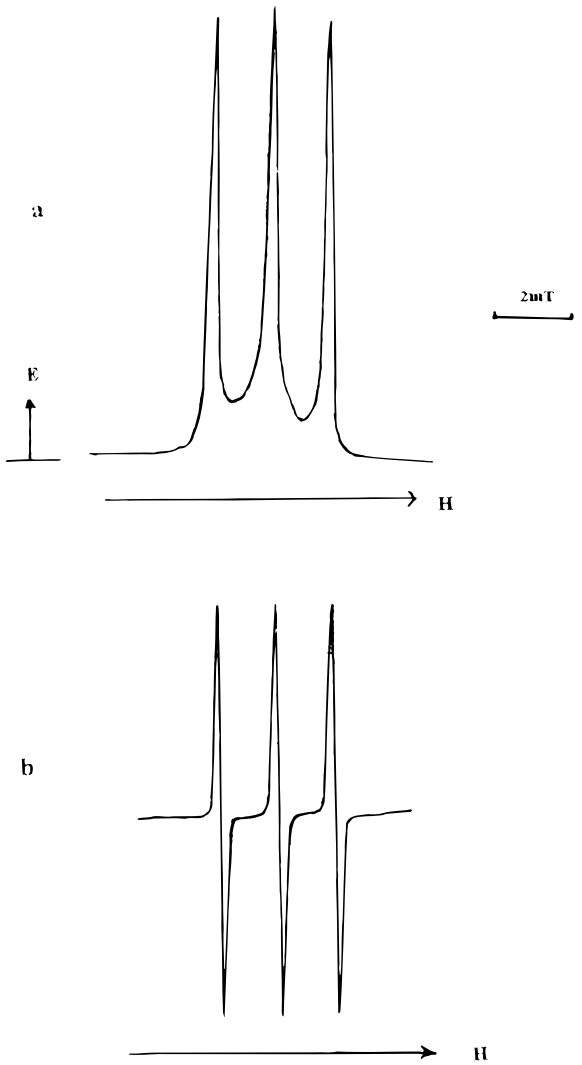

Figure 1. (a) CIDEP spectrum of PTH (26 mM) and TEMPO (10 mM) in ethylene glycol. The doorwidth of the boxcar was 299 ns; the delay time of the door opened after the laser flash was 2 μs. (b) Continuous wave ESR spectrum of TEMPO (10 mM) in ethylene glycol.

loscope for CIDEP decay profiles. Pure nitrogen gas was bubbled through the sample solutions prior to the measurements. The deoxygenated sample solutions were exposed to laser irradiation while flowing through a flat quartz cell (0.3 mm optical path length) in the ESR cavity with a flow rate of 9 mL/min. All TRESR measurements were carried out at room temperature.

The nonradiative and triplet quantum yield were determined by using a pulsed laser photoacoustic calorimeter, which has been described elsewhere.[18] It consisted of the above-mentioned Nd:YAG laser or N_2 laser (337 nm, 20 ns pulse width, 10 mJ/pulse energy, 10 Hz repetition frequency), a self-made photoacoustic transducer and an amplifier, and a digital oscilloscope (HP-5460) connected to a microcomputer (486-50) through a RS 232-interface. The laser energy was kept below 100 μJ/pulse to avoid any nonlinear effects in the illuminated sample solutions. Absorbance (A) of samples or reference compounds was determined by using a Hitachi-340 spectrometer. The fluorescence spectrum and fluorescence quantum yield (Φ_f) were determined by using a Hitachi-MPF-4 fluorescence spectrometer. The excitation wavelength was at 350 nm. Rhodamine 6G (Φ_f = 0.95) was used as reference to determine the fluorescence quantum yield of phenothiazine.[19]

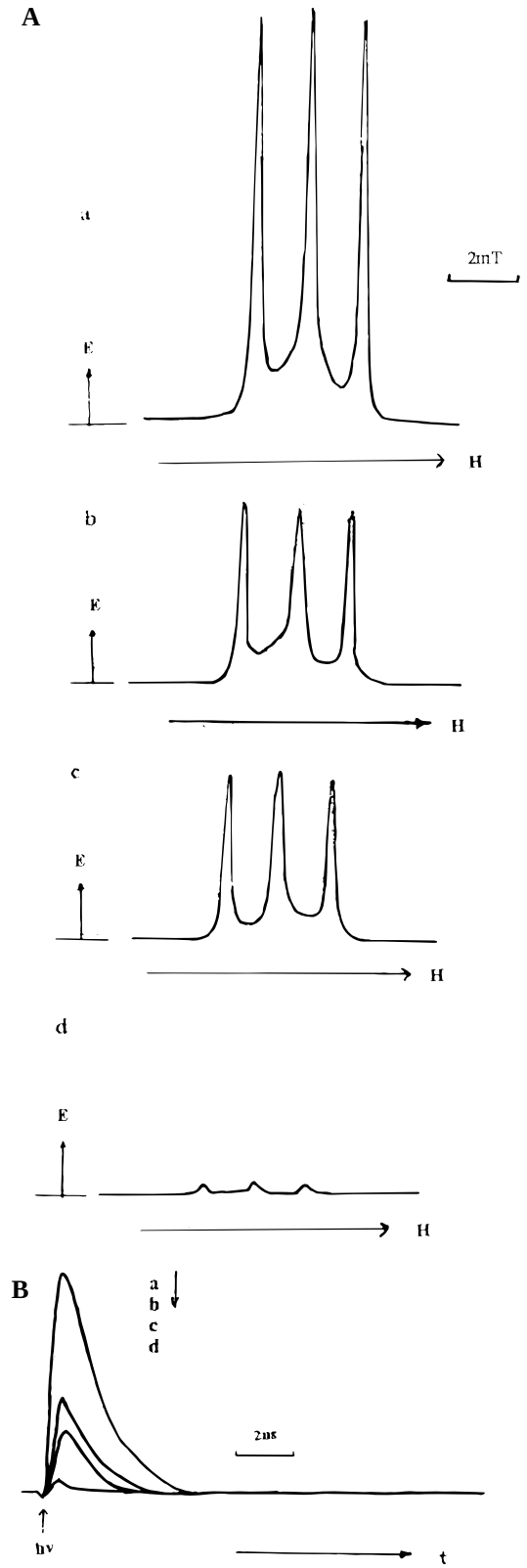

Figure 2. CIDEP spectra (A) and the time profile (m_1 = 0) (B) of PTH (26 mM) and TEMPO (10 mM) in an ethylene glycol (mL)/acetonitril (mL) mixture solvent: (a) 30/0, (b) 29/1, (c) 25/5, (d) 20/10.

3. Results and Discussion

3.1. TRESR. Before irradiation with the 355 nm laser beam neither the PTH−TEMPO−RH, PTH−RH, nor the TEMPO−RH system gave CTDEP signals. However, Figure 1a shows the TRESRS obtained after irradiation with the 355 nm laser

TABLE 1: Values of A and K for the Time Profiles ($m_1 = 0$) of the PTH (26 mM) and TEMPO (10 mM) System in Different Solvent Mixtures

ethylene glycol/acetonitrile (mL/mL)	K_1^{-1} (μs)	K_2^{-1} (μs)	A_1	A_2
30/0	1.4	169.3	42.1	7.2
29/1	0.3	63.1	7.1	1.2
25/5	0.2	8.2×10^{-3}	2.2	0.2
20/10				

beam in the PTH−TEMPO−RH system. The spectrum appears as a triplet hyperfine structure with emissive CIDEP signals. The hyperfine structure is the same as that of the CW ESR spectrum of TEMPO with three peaks of equivalent intensity corresponding to the nuclear spin states of the nitrogen atom, as shown in Figure lb. Therefore the observed CIDEP signals can be assigned to the polarized TEMPO radical.

It is known that TEMPO cannot be excited by the 355 nm laser beam and PTH can be excited by 355 nm light; its triplet quantum yield Φ_T measured from pulse laser photoacoustic calorimetric technique is 0.86.[20] Therefore it is rational to explain the emissive CIDEP pattern of TEMPO in terms of the radical−triplet pair mechanism,[8] that is, the triple−doublet encounter complex (^{3}PTH−^{2}R) (^{2}R = TEMPO) formed by photogenerated triplet-state molecules ^{3}PTH and doublet-state radicals TEMPO. Those encounter complexes may be either a quartet or a doublet pair spin state. The doublet encounters can undergo triplet quenching, and the radicals will leave those encounters unpolarized as follows:

$$^2(^3\text{PTH}-^2\text{R}) \xrightarrow{\text{quenching}} {}^2(^1\text{PTH}_0-^2\text{R})$$

$$^2(^1\text{PTH}_0-^2\text{R}) \rightarrow {}^1\text{PTH}_0 + {}^2\text{R}$$

On the other hand, the quartet state of the radical−triplet pairs $^4(^3$PTH−^{2}R) are expected to survive through spin triplet quenching. The remaining quartet pair states experience radical−triplet interactions, altering the spin state populations with time. If quartet−doublet mixing by the zero-field splitting (zfs) and quartet−doublet splitting by the exchange interaction are considered, the resulting radical spin polarization $\langle S_{Rz}\rangle$ should roughly follow the proportionality[8]

$$\langle S_{Rz}\rangle \propto \omega J D^2$$

where ω is the microwave frequency, $J = E$(doublet) − E(quartet), the exchange interaction, and $|D| = 0.1296$ cm^{-1} is the dominating zfs parameter of ^{3}PTH.[2l] Thus from the observed emissive CIDEP signals as shown in Figure la, the J value should be positive. Because the multiplet polarization in Figure 1 is not clear, we neglect the effect of the hyperfine interaction H_{hfs}

If we consider the time dependencies of $J(t)$ and $H_{zfs}(t)$, the RTPM polarization should increase with increasing solvent viscosity.[8] Therefore the CIDEP spectra obtained in different viscous solutions in the PTH−TEMPO system as shown in Figure 2 is expected. The time profiles in Figure 2 can be expressed by the following equation:

$$P(t) = A_1 \exp(-K_1 t) + A_2 \exp(-K_2 t) \quad (1)$$

The constants A and K obtained by fitting the equation with experimental time profiles are listed in Table 1.

3.2. Fluorescence Quenching Measurement. The fluorescence spectra obtained for PTH in the absence and presence of TEMPO were shown in Figure 3. The plot of the ratio of the fluorescence intensity F_0 in the absence of TEMPO to F in the presence of TEMPO against the concentration of TEMPO as shown in Figure 4 is a straight line. Therefore it obeys the Stern−Volmer equation.[22]

$$F_0/F = 1 + K[\text{TEMPO}] \quad (2)$$

$$= 1 + K_q \tau_0 [\text{TEMPO}] \quad (3)$$

where K and K_q are the Stern−Volmer quenching constant and bimolecular quenching constant, respectively. τ_0 is the fluorescence lifetime of PTH in the absence of TEMPO. The values of K and K_q obtained from the measured slope and the value of τ_0 previously published[23] are listed in Table 2. It is known that τ_0 is dependent on the viscosity of solvent and τ is dependent on the concentration of TEMPO.[23] Consequently, we can predicate the quenching process must be a dynamic quenching.[22]

3.3. Effect of TEMPO on the Nonirradiative Quantum Yield Φ_{nr} of PTH. The relationship between experimentally measured photoacoustic signal V_{pa} and nonirradiative quantum yield Φ_{nr} is expressed as[18,19,23−26]

$$V_{pa} = K\Phi_{nr}E_L(1 - 10^{-A}) \quad (4)$$

For low concentration

$$V_{pa} \cong K\Phi_{nr}E_L A \quad (5)$$

where K is a constant that depends on the geometry of the experimental setup and the thermoplastic quantities of the medium. Here E_L is the incident laser pulse energy, and Φ_{nr} is the fraction of laser energy absorbed by PTH released nonradiatively as the thermal energy within the response time of the detector of the photoacoustic calorimeter. A is the absorbance (or optic density) of the sample solution.

By measuring V_{pa} under identical conditions for PTH in ethylene glycol solution in the presence of TEMPO and reference (anthrancene) with known Φ_{nr} in ethylene glycol solution and from the ratio of the slope of V_{pa} versus A for PTH in the presence of TEMPO to that for anthrancene as shown in Figure 5, the Φ_{nr} of PTH in the presence of TEMPO obtained from eq 6 is listed in Table 3.

$$\Phi_{nr}(\text{sample}) = \text{slope(sample)} \times \Phi_{nr}(\text{reference})/\text{slope (reference)} \quad (6)$$

It is obvious that the Φ_{nr} of PTH in the presence of TEMPO is larger than that of PTH in the absence of TEMPO. If we examine Figure 3, it is found that, after addition of 1 mM, 2 mM, and 3 mM TEMPO into 3×10^{-4} M PTH in ethylene glycol solution, the fluorescence intensity F (or fluorescence quantum yield Φ_f) of ^{1}PTH in the presence of TEMPO decreases to $0.97F_0$ ($0.97\Phi_f^0$), $0.91F_0$ ($0.91\Phi_f^0$), and $0.87F_0$ ($0.987\Phi_f^0$), respectively.

Now we examine through what pathway the fluorescence intensity F (or fluorescence quantum yield Φ_f) or the nonradiative quantum yield Φ_{nr} may be decreased or increased in detail in the following cases.

Case 1. The decreased fluorescence quantum yield is completely converted into the form of thermal energy and released immediately to the medium, and ^{3}PTH is not quenched

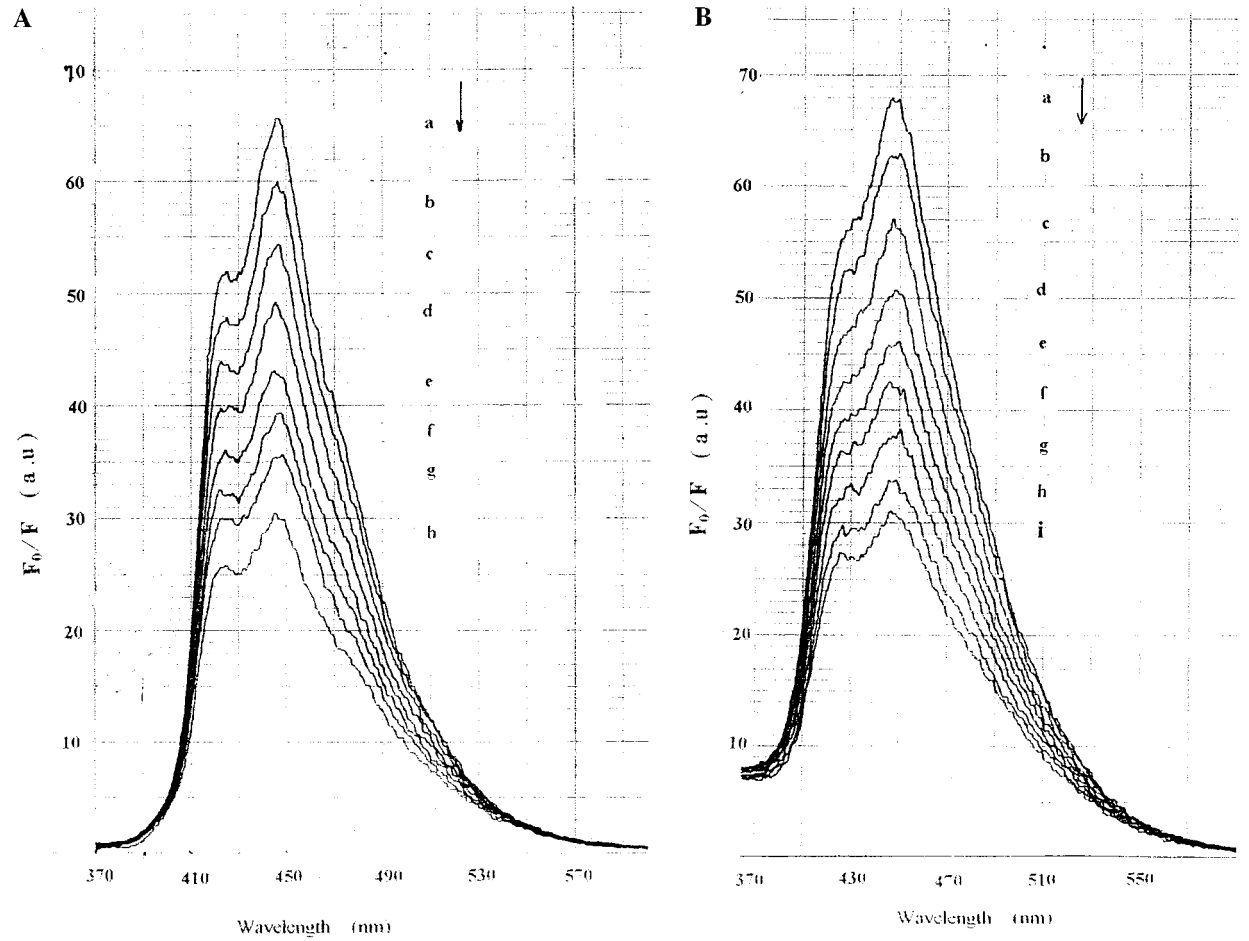

Figure 3. (A) Fluorescence spectra of PTH (3.5×10^{-4} M) in 2-propanol at various concentrations of TEMPO: (a) 0 mM, (b) 2.7 mM, (c) 6.40 mM, (d) 10.20 mM, (e) 14.60 mM, (f) 18.80 mM, (g) 23.40 mM, (h) 28.40 mM. (B) Fluorescence spectra of PTH (3.5×10^{-4}) in ethylene glycol at various concentrations of TEMPO: (a) 0 mM, (b) 2.5 mM, (c) 5.6 mM, (d) 8.7 mM, (e) 11.50 mM, (f) 14.50 mM, (g) 18.00 mM, (h) 21.30 mM, (i) 24.00 mM.

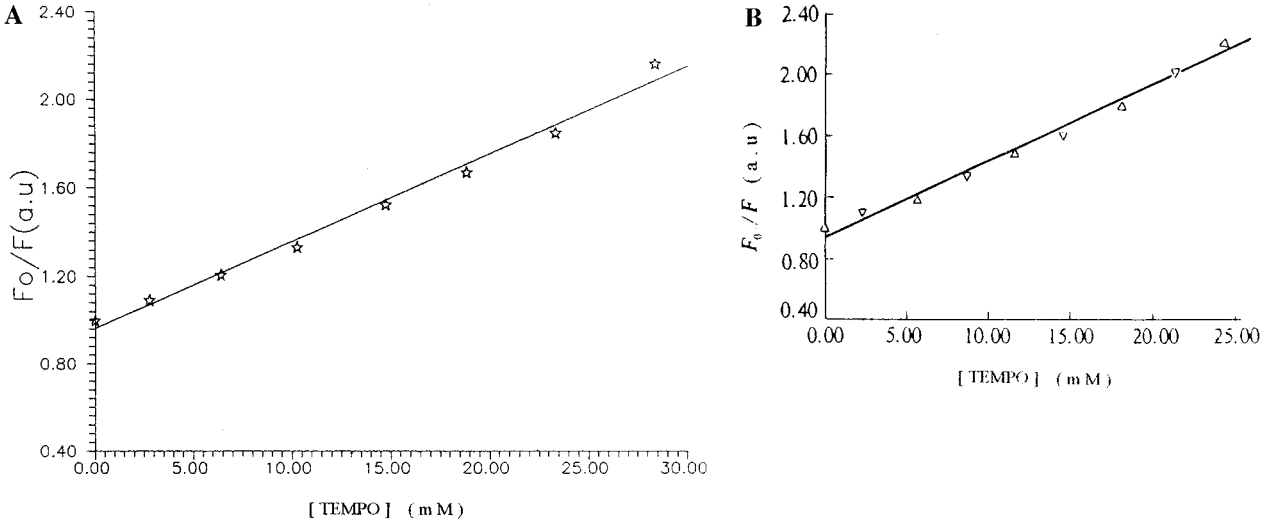

Figure 4. Plots of the ratio F_0/F against [TEMPO] for PTH in 2-propanol (A) and in ethylene glycol (B).

by TEMPO. Then the Φ_{nr} of PTH in the presence of TEMPO obtained by the following energy balance eq 7[25,26] is about 0.21−0.22. It is in disagreement with the measured one, $\Phi_{nr} = 0.70$.

$$\Phi_{nr} = 1 - \Phi_f' h\nu_f/E_L - \Phi_T E_T/E_L \qquad (7)$$

where the term $\Phi_f' h\nu_f/E_L$ represents the fraction of absorbed energy emitted in the form of fluorescence in the presence of TEMPO and the term $\Phi_T E_T/E_L$ represents the fraction of absorbed energy stored in triplet-state ^{3}PTH. E_T and Φ_T are the energy and quantum yield of ^{3}PTH, respectively.

Case 2. The decreased fluorescence quantum yield ($\Phi_f^0 - \Phi_f'$) is equal to the increased triplet quantum yield ($\Phi_T' - \Phi_T$) of ^{3}PTH, and ^{3}PTH is not quenched by TEMPO. Hence the Φ_{nr} in the presence of TEMPO obtained by the following energy

TABLE 2: Quenching of PTH Fluorescence by TEMPO

solvent	viscosity	K (M^{-1})	τ_0^{23} (ns)	τ^{*23} (ns)	K_q (M^{-1} s^{-1})
2-propanol	2.86	39.5	7.31		5.4
ethylene glycol	19.9	48.8	19.52		2.5
				3.56[a]	
				2.57[b]	
				1.53[c]	

[a] The fluorescence lifetime of PTH (3.5×10^{-4} M) in ethylene glycol at a concentration of TEMPO of 5.66 mM. [b] At a concentration of 14.60 mM. [c] At a concentration of 21.26 mM.

balance eq 8 is about 0.18−0.20. It is also not consistent with the measured one ($\Phi_{nr} = 0.70$).

$$\Phi_{nr} = 1 - \Phi_f' h\nu_f/E_L - (\Phi_T + \Phi_f^0 - \Phi_f')E_T/E_L \quad (8)$$

Case 3. The decreased fluorescence quantum yield is completely converted into thermal energy and ^{3}PTH is completely quenched by TEMPO. Then the Φ_{nr} of ^{3}PTH in the presence of TEMPO obtained by following eq 9 is about 0.82−0.84. It is approximately the same as the measured one ($\Phi_{nr} = 0.70$).

$$\Phi_{nr} = 1 - \Phi_f' h\nu_f/E_L \quad (9)$$

On the basis of the above discussion, it is clear that ^{3}PTH is quenched by TEMPO, and this provides direct evidence for the selective triplet quenching in RTPM proposed by Blätter et al.[8]

The overall photoinduced reaction mechanism may be described as follows:

$$^1\text{PTH}_0 \xrightarrow{h\nu} {}^1\text{PTH}$$

$$^1\text{PTH} \xrightarrow{kr} {}^1\text{PTH}_0 + h\nu_f$$

$$^1\text{PTH} \xrightarrow{kir} {}^1\text{PTH}_0$$

$$^1\text{PTH} + {}^2\text{R} \rightarrow {}^2\overline{(^1\text{PTH}-{}^2\text{R})}$$

$${}^2\overline{(^1\text{PTH}-{}^2\text{R})} \xrightarrow{\text{ISC}} {}^{2,4}\overline{(^3\text{PTH}-{}^2\text{R})}$$

$$^1\text{PTH} \xrightarrow{k_{ISC}} {}^3\text{PTH}$$

$$^3\text{PTH} + {}^2\text{R} \rightarrow {}^{2,4}\overline{(^3\text{PTH}-{}^2\text{R})}$$

$${}^2\overline{(^3\text{PTH}-{}^2\text{R})} \xrightarrow{\text{ISC}} {}^2\overline{(^1\text{PTH}_0-{}^2\text{R})} \rightarrow {}^1\text{PTH}_0 + {}^2\text{R}$$

$${}^4\overline{(^3\text{PTH}-{}^2\text{R})} \rightarrow {}^1\text{PTH}_0{}^* + {}^2\text{R}^*$$

It is evident that two kinds of complexes, (^{1}PTH−^{2}R) and (^{3}PTH−^{2}R), may be formed; the former is caused by the frequent collision of ^{2}R (TEMPO) with ^{1}PTH and the latter arising from the random encounter of ^{3}PTH* with TEMPO is dominate or, when produced by enhanced ISC of (^{1}PTH−^{2}R), is sparse and can be neglected in our experiment.

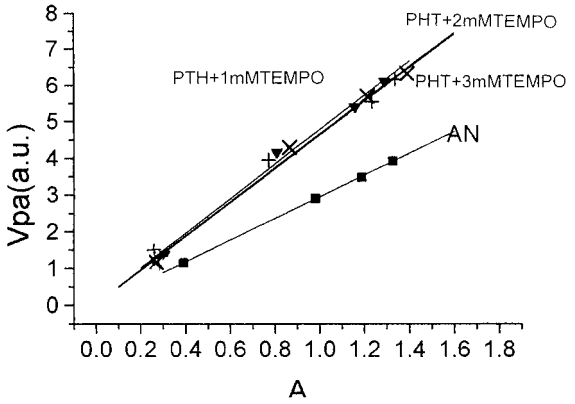

Figure 5. Linear dependence of the V_{pa} (au) signal on the absorbance A for the optical path length $L = 10^{-2}$ cm for anthracene (AN, ■) in ethylene glycol and PTH in ethylene glycol in the presence of TEMPO (1 mM, ×; 2 mM, ▼; 3 mM, +), respectively.

TABLE 3: Φ_{nr} and Φ_T of Phenothiazine Determined by Photoacoustic Calorimetric Measurement

compound	solvent	Φ_f	$h\nu_f$ (cm^{-1})	E_T	Φ_{nr}	Φ_T
anthracene	ethylene glycol	0.27	24 000	14 900	0.44	0.66
acridine	ethylene glycol	0.20	23 250	15 580	0.47	0.82
PTH	ethylene glycol	0.24	22 483	21 503	0.19[20]	0.86[20]
PTH+TEMPO	ethylene glycol				0.70	

Acknowledgment. This project (no. 29773050) is supported by the National Natural Science Foundation of China.

References and Notes

(1) Fessenden, R. W.; Schuler. *J. Chem. Phys.* **1963**, *39*, 2147.
(2) Hore, P. J.; Joslin, C. G.; McLauchlan, K. A. *Chem. Soc. Rev.* **1979**, *8*, 29.
(3) McLauchlan, K. A. In *Modern Pulsed and Continuous-Wave Electron Spin Resonance*; Kevan, L., Bowman, M. K., Eds.; John Wiley & Sons Inc.: New York, 1990.
(4) Wong, S. K.; Wan, J. K. S. *J. Am. Chem. Soc.* **1972**, *94*, 7197.
(5) Adrin, F. J. *Rev. Chem. Intermed.* **1979**, *3*, 3.
(6) Muus, L. T.; Atkins, P. W.; McLauchlan, K. A.; Pedersen, J. B. *Chemically Induced Magnetic Polarization*; Reidel: Dordrecht, 1977.
(7) Salikhov, K. M.; Molin, Yu. N.; Sagdeev, R. Z.; Buchachenlo, A. L. *Spin Polarization and Magnetic Field Effects in Radical Reactions*; Elsevier: New York, 1984.
(8) Blätter, C.; Jent, F.; Paul, H. *Chem. Phys. Lett.* **1990**, *166*, 375.
(9) Kawai, A.; Qkutsu, T.; Obi, K. *J. Phys. Chem.* **1991**, *95*, 9130.
(10) Kawai, A.; Obi, K. *J. Phys. Chem.* **1992**, *96*, 52.
(11) Kobori, Y.; Kawai, A.; Obi, K. J *Phys. Chem.* **1994**, *98*, 6425.
(12) Green, J. A.; Singer, L. A. *J. Chem. Phys.* **1971**, *58*, 2690.
(13) Watkins, A. R. *Chem. Phys. Lett.* **1974**, *29*, 526.
(14) Kumin, V. A.; Tatikolov, A. S. *Chem. Phys. Lett.* **1978**, *53*, 606.
(15) Schwerzel, R. E.; Caldwell, R. A. *J. Am. Chem. Soc.* **1973**, *95*, 1382.
(16) Tachikawa, H.; Bard, A. J. *Chem. Phys. Lett.* **1974**, *26*, 10.
(17) He, G. L.; Fu, L. Y.; Lu, T. X.; Xu, G. Z. *Chin. Sci. Bull.* **1996**, *41*, 1389.
(18) Song, X. Q.; Zhang, Y. K.; Xu, G. Z. *Chin. Sci. Bull.* **1991**, *36*, 1000.
(19) Rothberg, L. J.; Simon, J. D.; Bernstein, M.; Peter, K. S. *J. Am. Chem. Soc.* **1983**, *105*, 3464.
(20) He, G. L.; Li, X. Y.; Yang, J. L.; Chen, C. P.; Xu, G. Z. *J. Photochem. Photobiol. A: Chem.* **1997**, *108*, 155.
(21) Weir, D. J.; Depew, M. C.; Wan, J. K. S. *Res. Chem. Intermed.* **1990**, *14*, 269.
(22) Lakowicz, J. R. *Principles of Fluorescence Spectroscopy*; Plenum Press: New York, 1983.
(23) Yang, J. L.; He, G. L.; Xu, G. Z. *Chin. Sci. Bull.* **1996**, *41*, 608.
(24) Scaiano, J. C.; Chen, C. P.; McGany, P. F. *J. Photochem. Photobiol. A: Chem.* **1991**, *62*, 75.
(25) Komonowski, S. J.; Grabowski, Z. P.; Zielenkiewicz, W. *J. Photochem.* **1985**, *30*, 141.
(26) Braskavsky, S. E.; Heibel, G. E. *Chem. Rev.* **1992**, *92*, 1381.